Microwave-Enhanced Synthesis of Cu_3Se_2 Nanoplates and Assembly of Photovoltaic CdTe−Cu_3Se_2 Clusters

Xuebo Cao,* Cui Zhao, Xianmei Lan, Geijian Gao, Wenhu Qian, and Yang Guo

Key Lab of Organic Synthesis of Jiangsu Province and Department of Chemistry, Suzhou University, Suzhou, Jiangsu 215123, People's Republic of China

Received: January 11, 2007; In Final Form: March 7, 2007

High-quality Cu_3Se_2 nanoplates were synthesized in a large scale through microwave-enhanced reaction between selenium and copper(I) oleate. The nanoplates are approximately round with thickness of 17 nm and the diameter in the range of 700∼1000 nm. The distinct shape of the nanoplates provides an ideal site for combining functional units, and as an example, carboxyl-terminated CdTe quantum dots were adsorbed onto Cu_3Se_2 nanoplates to form Cu_3Se_2−CdTe nanocluster by the chemical linkage of carboxyl to Cu. The fabricated nanoclusters exhibit an enhanced photovoltaic property (i.e., large photocurrent and short response time). Furthermore, this work provides a rational method to the design and fabrication of quantum dots decorated semiconductor nanocomposites.

Introduction

During recent decades, a remarkable success has been achieved in growing single-component nanocrystals with controlled dimensions and intriguing morphologies. Now, the studies on the fabrication of heterogeneous nanostructures consisting of discrete domains of different materials have been motivated increasingly,[1] since nanocomposite materials provide the possibility for the nanoscale integration of the functionality of every component within them. Generally, multicomponent nanostructures exhibit enhanced functionality, multifunctional properties, and even some new properties in contrast with their more limited single-component counterparts.[2] Of various composite nanostructures, the "coupled" type nanocomposites constructed by two semiconductors, such as CdS/TiO_2,[3] Cd_3P_2/ZnO,[4] AgI/TiO_2,[5] and so on,[6] are particularly interesting in highly efficient photoelectrical conversion. The photogenerated carriers in the coupled type semiconductor nanocomposites can inject from one to the other, which blocks the recombination of electrons and holes and will result in an efficient separation of charges.

Copper selenides, existing in diverse phases and structural forms as stoichiometric Cu_2Se, Cu_3Se_2, CuSe, and $CuSe_2$ and nonstoichiometric $Cu_{2-x}Se$,[7] are conventional semiconductors applied in solar cells,[8] optical filters,[9] and optoelectronics devices.[10] However, the photovoltaic properties of single copper selenides is not satisfying, and hence, copper selenides are usually combined with indium selenides to form ternary compound $CuInSe_2$ to achieve high conversion efficiency.[11] CdTe is another fascinating photovoltaic material because its relatively high optical absorption coefficient ($>10^4$ cm^{-1}) imparts it the characteristic that a very thin layer CdTe can absorb the great mass of visible light (around 90%).[12] Especially for quantum-sized CdTe, because of the quantum confinement of charge carriers in tiny spaces, it possesses more excellent and tunable optical and electrical properties.[13] A fatal deficiency of CdTe as a photovoltaic material is that the photogenerated charges are inclined to recombine immediately within the surface layer.[14] Because of the efficient separation of photogenerated charges in the composite nanostructures, the coupling of CdTe to copper selenides should be an efficient approach to solve the problem. In addition, CdTe and copper selenides are both photovoltaic, and hence, the combination of them can achieve collective properties. To date, there have been no attempts devoted to the fabrication of such a nanostructure.

In this paper, we first prepared high-quality nanoplates of stoichiometric copper selenide (Cu_3Se_2) via a microwave-enhanced route. Then, using Cu_3Se_2 nanoplates and CdTe quantum dots (QDs) stabilized by thioglycollic acid (TGA) as building blocks, we successfully fabricated CdTe−Cu_3Se_2 clusters by means of the good affinity of carboxyl groups to transition-metal ions.[15] As expected, the assembled CdTe−Cu_3Se_2 clusters actually exhibit good optical and photovoltaic properties.

Experimental Section

Preparation of Cu_3Se_2 Nanoplates. All the chemical reagents were of analytical grade (Shanghai Chemical Reagent Corp.) and were used as received. Copper(I) oleate was prepared according to Choi et al.[16] In a typical process, 0.079 g selenium powders (1 mmol), 0.365 g copper(I) oleate (1 mmol), and 50 mL *N*,*N*-dimethylformamide were put into a 100 mL quartz flask. The flask was then placed into Sino MSZ-1 microwave reactor (Frequency: 2450 MHz) equipped with a magnetic stirrer and a water-cooled condenser. After purging by nitrogen for 30 min, the temperature of the system was increased to 100 °C and the system was irradiated for 60 min. Black solids were separated from the solution by centrifugation and were washed three times with 50 mL distilled water. The products were dried in vacuum at 40 °C for 6 h.

Coupling CdTe Quantum Dots to Cu_3Se_2 Nanoplates. CdTe quantum dots stabilized by TGA were synthesized according to the description by Zhang et al.[17] To prepare CdTe−Cu_3Se_2 clusters, 0.05 g of Cu_3Se_2 nanoplates was dispersed into

* To whom correspondence should be addressed. E-mail: xbcao@suda.edu.cn.

10.1021/jp0702301 CCC: $37.00 © 2007 American Chemical Society
Published on Web 04/13/2007

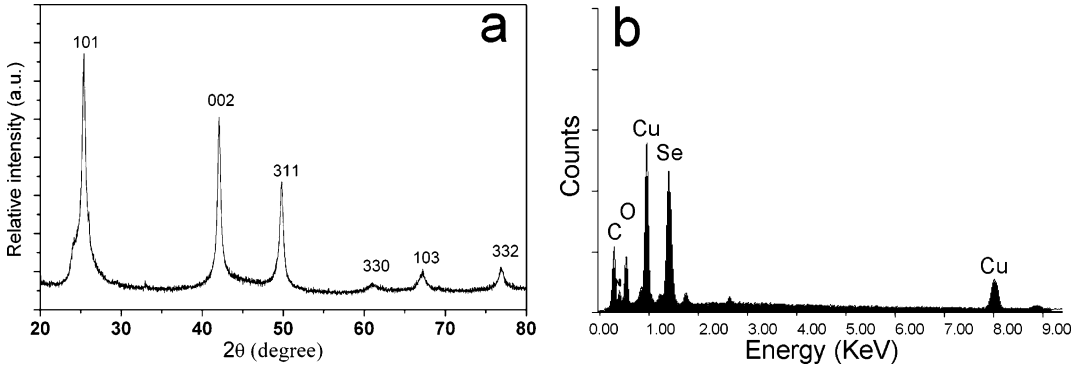

Figure 1. (a) XRD pattern of Cu_3Se_2 nanoplates. (b) EDAX spectrum of Cu_3Se_2 nanoplates.

10 mL distilled water by ultrasonic. Then, 5 mL aqueous solution containing CdTe quantum dots (0.01 mol/L) was added into the solution of Cu_3Se_2 nanoplates. After stirring at room temperature for 12 h, the solid product was separated by centrifugation at 2500 rpm and was washed three times with 60 mL distilled water to remove uncombined CdTe quantum dots.

Characterization of Structures, Morphologies, and Properties of Cu_3Se_2 Nanoplates and CdTe−Cu_3Se_2 Clusters. X-ray powder diffraction (XRD) patterns of the products were recorded on an X'Pert PRO SUPER rA rotation anode X-ray diffractometer with Ni-filtered Cu Kα radiation ($\lambda = 1.54178$ Å). Transmission electron microscopy (TEM) measurements were carried out on an FEI Tecnai G20 electron microscope, using an accelerating voltage of 160 kV. High-resolution transmission electron microscopy (HRTEM) images and selected area electron diffraction (SAED) patterns were taken on a JEOL-2010 TEM at an acceleration voltage of 200 kV. Scanning electron microscopy images were taken on a HITACHI S-4700 field-emitting scanning electron microscope (FESEM). EDAX measurements were performed with the energy-dispersive X-ray (EDAX) spectrometer attached on the HITACHI S-4700 FESEM. Optical absorption spectra were recorded on a Shimadzu 3150 UV−vis−near-infrared spectrophotometer. The photocurrent measurements were carried out in aqueous Na_2SO_4 solution by a conventional three-electrode photoelectrochemical cell, where the counter, reference, and working electrodes are platinum, Ag/AgCl, and indium−tin−oxide (ITO) substrate (area: 1 cm^2) deposited by CdTe−Cu_3Se_2 clusters, pure Cu_3Se_2 nanoplates, or CdTe quantum dots. The illumination was provided by a 250 W Xe lamp.

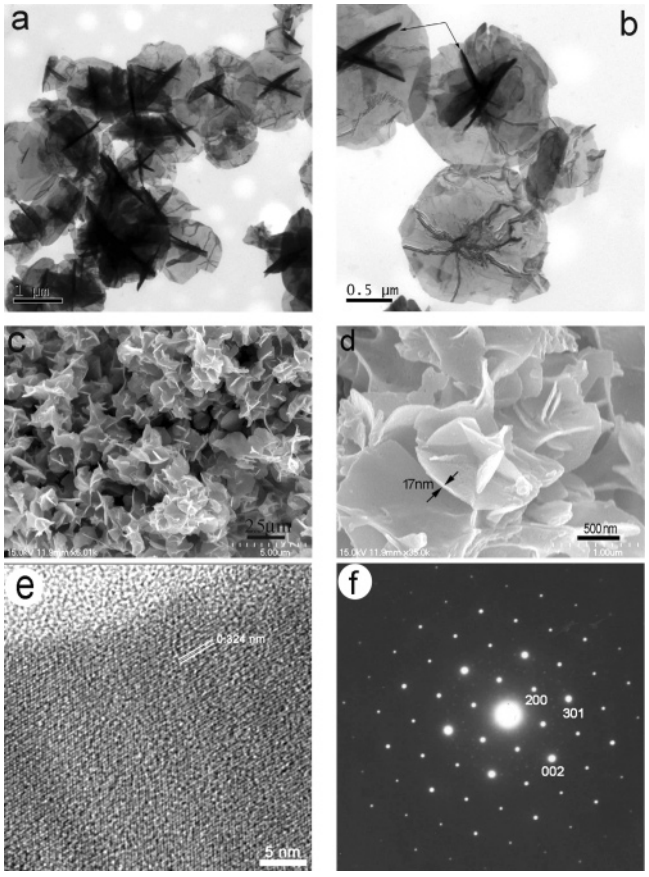

Figure 2. (a, b) TEM images of Cu_3Se_2 nanoplates. (c, d) FESEM images of Cu_3Se_2 nanoplates. (e) HRTEM images of Cu_3Se_2 nanoplates. (f) SAED pattern taken on a single Cu_3Se_2 nanoplate.

Results and Discussion

Figure 1a displays the XRD pattern of the as-prepared copper selenides via the microwave-enhanced route. The index of the six reflections reveals that the product is composed of tetragonal Cu_3Se_2 (JCPDS file, No. 72-1421). No impurities such as elemental selenium and copper oxides are detected. The calculated lattice constants $a = 6.408$ Å and $c = 4.283$ Å are well consistent with the standard literature data ($a = 6.406$ Å and $c = 4.279$ Å). The strong and wide features of the reflections are related to the small size and the good crystallinity of the product. Furthermore, in comparison with the standard XRD pattern of Cu_3Se_2, parts of peaks are absent and the reflection from (002) planes is abnormally strong in the spectrum of our product, which suggests that the product possesses a good orientation parallel or perpendicular to the *c*-axis. Figure 1b exhibits the EDAX spectrum measured using the spectrometer attached on an FESEM, which confirms that the product is composed of Cu_3Se_2 because the detected Cu and Se are in a molar ratio of 1.47:1. The signals of O and C should be attributed to the use of copper(I) oleate, which results in the adsorption of oleates onto the surface of Cu_3Se_2 nanoplates. The signal of silicon arises from the silicon substrate onto which the sample is deposited.

Figure 2a−d depicts the morphology of the as-prepared Cu_3Se_2 nanocrystals via the microwave-enhanced route. From the TEM and FESEM images, it can be seen that the product is composed of approximately round nanoplate in an extremely high yield (almost 100%). According to TEM images, the surface of the nanoplates is very clean, and the diameters of the nanoplates are determined to be in the range of 700∼1000 nm. The nearly transparent feature of the nanoplates suggests that they should be very thin in thickness. FESEM studies confirm this presumption, and the measurements on 100 nanoplates reveal that the average thickness of the nanoplates is around 17 nm. Interestingly, parts of the plates are penetrating

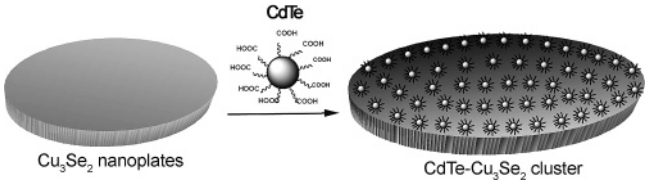

Figure 3. Schematic diagram of the assembly of CdTe−Cu_3Se_2 clusters through the chemical linkage of CdTe QDs to Cu_3Se_2 nanoplates.

each other, which could account for the black lines found in TEM images, as indicated by arrows in Figure 2b. The as-prepared Cu_3Se_2 nanoplates are particularly suitable for the construction of nanocomposites because their wide and flat surface provides ideal sites for holding functional units (e.g., CdTe QDs) with a high content.

Figure 2e shows the HRTEM image of the Cu_3Se_2 nanoplate. The clearly observed lattice fringes indicate that the Cu_3Se_2 nanoplates are highly crystalline. The resolved interplanar spacing is 3.24 Å, corresponding to the separation between the (200) lattice planes of tetragonal Cu_3Se_2. Figure 2f is the typical SAED pattern recorded with the incident electron beam perpendicular to the surface of single Cu_3Se_2 nanoplate. The 2-fold symmetric spots demonstrate that the nanoplates are single crystalline in structure and the index of the pattern demonstrates that it matches the tetragonal Cu_3Se_2 structure well. In addition, in combination with the results of HRTEM and SAED, it can be deduced that the wide surface of the nanoplate is terminated by the (002) crystallographic plane. As mentioned above, this preferential growth results in the abnormal strength of the (002) plane that is found in the studies of XRD.

The formation of Cu_3Se_2 nanoplates with an extremely high yield is at least related to three factors. The first factor is that, in the microwave field, selenium powders and copper(I) oleates show a large solubility in the alkaline solvent of *N*,*N*-dimethyl formamide at 100 °C, and thus, a homogeneous reaction takes place between them, which is indispensable for the homogeneous growth of regular nanocrystals. Theoretically speaking, the reaction between copper(I) oleate and selenium should produce copper(I) selenide such as $Cu_{2-x}Se$ or Cu_2Se. However, $Cu_{2-x}Se$ phase can get converted to the Cu_3Se_2 phase at a low temperature (<140 °C) because the former is less stable under such conditions.[18] The second factor is that microwave heating is highly efficient and has no thermal gradient effects, which favors the humongous nucleation on a large scale and eventually leads to the formation of products with an extremely high yield.[19] The third factor is the participation of oleate in the growth process of Cu_3Se_2 nanoplates because oleate is a particularly efficient group in the morphology-controlled growth of inorganic nanocrystals.[16,20] Anionic oleates are inclined to selectively bind onto the positively charged Cu-terminated (001) surfaces, and hence, the growth along the *c*-axis is suppressed. As a result, the product presents a platelike shape with their wide surface corresponding to (002) crystallographic planes.

The assembly of CdTe−Cu_3Se_2 clusters is based on the good affinity of carboxyl groups to transition-metal ions. Since the surface of CdTe QDs stabilized by TGA is terminated by a large number of carboxyl groups, they can be chemically adsorbed onto the surface of the nanoplate tightly through the interaction between carboxyl groups and Cu ions, as diagrammatically described in Figure 3. CdTe QDs for the assembly of CdTe−Cu_3Se_2 clusters have an average diameter of 4.1 nm in this study. Figure 4a shows the TEM image of the Cu_3Se_2 nanoplates after interacting with CdTe QDs. The surface of the nanoplate is covered by numerous CdTe QDs, and hence, their contrast is much stronger compared to that of pure Cu_3Se_2 nanoplates (Figure 1a and 1b), which demonstrates that CdTe−Cu_3Se_2 clusters are successfully prepared through the chemical linkage of CdTe quantum dots to Cu_3Se_2 nanoplates. Further studies by FESEM verify the existence of CdTe QDs on the surface of Cu_3Se_2 nanoplates. As shown in Figure 4b and 4c, FESEM images clearly demonstrate that the nanoplates lose their original smoothness and are coated by a monolayer of CdTe QDs. As a result, the thickness of the CdTe−Cu_3Se_2 clusters increases to 25 nm, a little larger than that of pure Cu_3Se_2 nanoplates. The chemical linkage between CdTe quantum dots and Cu_3Se_2 nanoplates is rather tight. Even suffering from violent ultrasound for 30 min, CdTe−Cu_3Se_2 clusters still maintain the composite structure well (Figure 4d). Besides the microscopy analysis of the CdTe−Cu_3Se_2 clusters, they are also assessed by XRD to learn their structure exactly (Figure 5). It can be seen that, besides those belonging to Cu_3Se_2, CdTe existing in the mixed phase of cubic and hexagonal structures is also detected, which supports the results of TEM and FESEM studies. The content of CdTe in CdTe−Cu_3Se_2 clusters is determined according to energy-dispersive spectroscopy. The chemical composition (in mass %) of CdTe−Cu_3Se_2 clusters is 6.82 (CdTe) and 93.18 (Cu_3Se_2).

Figure 6 shows the optical absorption spectra of CdTe−Cu_3Se_2 clusters, pure Cu_3Se_2 nanoplates, and CdTe QDs, all of which are background-corrected. Pure Cu_3Se_2 nanoplates show a much intense absorption in visible region and a weak absorption in ultraviolet region (Figure 6a). The absorption onset of the nanoplates is located at 691 nm, which is distinctly different from the absorption edge around 600 nm that is found in Cu_3Se_2 thin films.[18,21] Since the sample for measuring the spectra is aqueous suspending liquid, the large red shift for our products is speculated to link with the surface-scattering effects and with the interactions of the solvent molecules. Additionally, it is also possible that the unique shape of the nanoplates contributes to the red shift because the optical properties of semiconductor nanomaterials are largely dependent on their morphology. With coupling of CdTe QDs, the formed CdTe−Cu_3Se_2 clusters not only show an intense absorption in visible region but also in ultraviolet region (Figure 6b). By comparison of the absorption curves of Cu_3Se_2−CdTe clusters, CdTe quantum dots, and pure Cu_3Se_2 nanoplates, the strong absorption of Cu_3Se_2−CdTe clusters in the ultraviolet region is believed to originate the contribution of CdTe quantum dots. The enhanced absorption in ultraviolet region could increase photon numbers utilized for the photoelectrical conversion. As a reflection of their absorption features, the photovoltaic properties of CdTe−Cu_3Se_2 clusters are superior to that of pure Cu_3Se_2 nanoplates and CdTe QDs, as learned from the measurements of photocurrent−time curves (Figure 7). It can be seen that the photocurrent intensity generated by CdTe−Cu_3Se_2 clusters is much larger than that of Cu_3Se_2 nanoplates and CdTe QDs. In addition, CdTe−Cu_3Se_2 clusters need a shorter response time for reaching saturation photocurrent relative to that of Cu_3Se_2 nanoplates and CdTe QDs. These results demonstrate that the formation of CdTe−Cu_3Se_2 favors the rapid and efficient separation of photogenerated charges in them, and as a result, the electron density transferred to the ITO substrate is increased. The essential reason responsible for the improvement of the photovoltaic properties of CdTe−Cu_3Se_2 should be similar to what is described in other coupled type semiconductor nanocomposites,[3−6] that is, the electrons can inject from the semiconductor with a lower conduction band level to that with

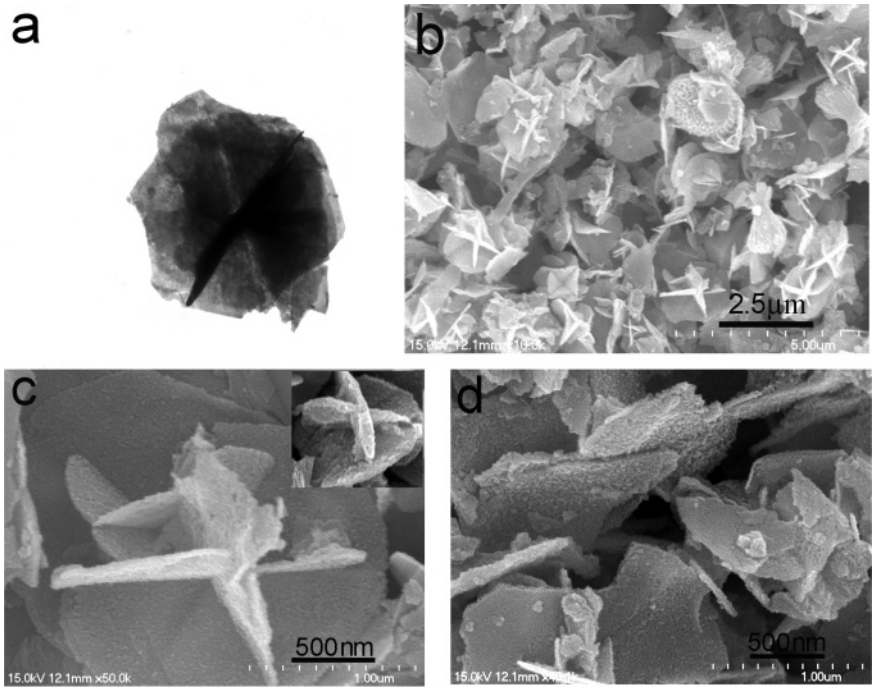

Figure 4. (a) TEM image of CdTe−Cu_3Se_2 clusters. (b, c) FESEM images of CdTe−Cu_3Se_2 clusters, where the inset shows a individual cluster. (d) FESEM image of CdTe−Cu_3Se_2 clusters suffering from violent ultrasonic dispersion, which reveals that the clusters still maintain their structures well.

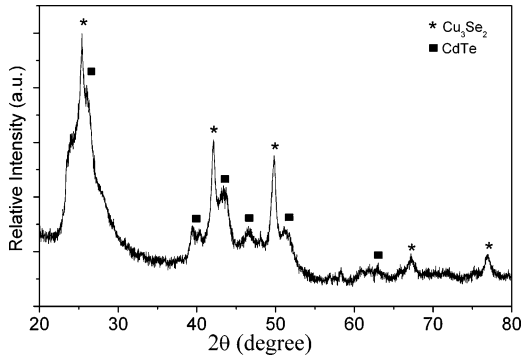

Figure 5. XRD pattern of CdTe−Cu_3Se_2 clusters.

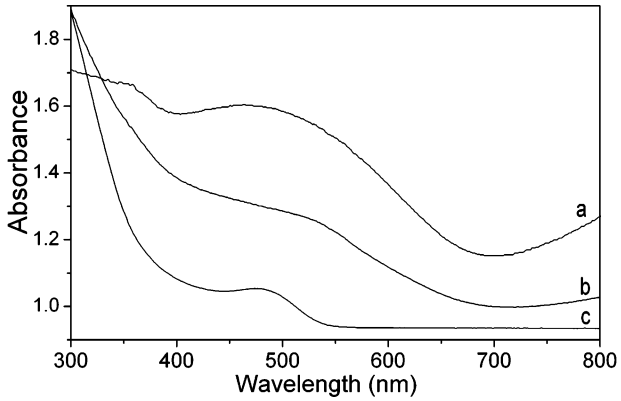

Figure 6. UV−vis absorption spectra: (a) Cu_3Se_2 nanoplates, (b) CdTe−Cu_3Se_2 clusters, and (c) CdTe QDs.

a high level, leading the flowing of the charges toward an opposite direction. Unfortunately, since there are no standard values found about the potentials of conduction band and valence band of Cu_3Se_2, we cannot distinguish the process of electron transfer in CdTe−Cu_3Se_2 clusters exactly.

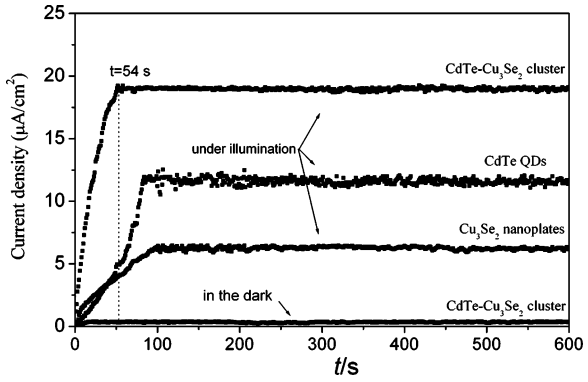

Figure 7. Photocurrent−time curves of Cu_3Se_2 nanoplates, CdTe quantum dots, and CdTe−Cu_3Se_2 clusters.

Conclusion

In summary, we have reported the microwave-enhanced synthesis of Cu_3Se_2 nanoplates and the assembly of CdTe−Cu_3Se_2 clusters by means of the chemical linkage of carboxyl groups to Cu ions, which should provide a rational method to the design and fabrication of QDs-decorated semiconductor nanocomposites. The CdTe−Cu_3Se_2 clusters exhibit improved optical and photoelectrical properties (large saturation photocurrent and short response time) relative to the single semiconductor, thereby confirming their potential applications in solar energy conversion and optoelectronics devices.

Acknowledgment. This work was financially supported by the Key Lab of Organic Synthesis of Jiangsu Province (P. R. China) and National Natural Science Foundation of China (20601020).

References and Notes

(1) (a) Mokari, T.; Rothenberg, E.; Popov, I.; Costi, R.; Banin, U. *Science* **2004**, *304*, 1787. (b) Paholski, C.; Kornowski, A.; Weller, H. *Angew.*

Chem., Int. Ed. **2004**, *43*, 4774. (c) Salgueirino-Maceira, V.; Correa-Duarte, M. A.; Farle, M.; Lopez-Quintela, A.; Sieradzki, K.; Diaz, R. *Chem. Mater.* **2006**, *18*, 2701. (d) Kim, H.; Achermann, M.; Balet, L. P.; Hollingsworth, J. A.; Klimov, V. I. *J. Am. Chem. Soc.* **2005**, *127*, 544. (e) Yang, J.; Elim, H. I.; Zhang, Q. B.; Lee, J. Y.; Ji, W. *J. Am. Chem. Soc.* **2006**, *128*, 6690. (f) Pellegrino, T.; Fiore, A.; Carlino, E.; Giannini, C.; Cozzoli, P. D.; Ciccarella, G.; Respaud, M.; Palmirotta, L.; Cingolani, R.; Manna, L. *J. Am. Chem. Soc.* **2006**, *128*, 6690.

(2) (a) Robel, I.; Bunker, B. A.; Kamat, P. V. *Adv. Mater.* **2005**, *17*, 2458. (b) Hirakawa, T.; Kamat, P. V. *J. Am. Chem. Soc.* **2005**, *127*, 3928. (c) Lin, H. Y.; Chen, Y. F.; Wu, J. G.; Wang, D. I.; Chen, C. C. *Appl. Phys. Lett.* **2006**, *88*, 161911. (d) Cao, X. B.; Gu, L.; Zhuge, L. J.; Gao, W. J.; Wang, W. C.; Wu, S. F. *Adv. Funct. Mater.* **2006**, *16*, 896.

(3) Lawless, D.; Kapoor, S.; Meisel, D. *J. Phys. Chem.* **1995**, *99*, 10329.

(4) Spanhel, L.; Henglein, A.; Weller, H. *Ber. Bunsenges. Phys. Chem.* **1987**, *91*, 1359.

(5) Fitzmaurice, D.; Frei, H.; Rabani, J. *J. Phys. Chem.* **1995**, *99*, 9176.

(6) Kryukov, A. I.; Kuchmii, S. Y.; Pokhodenko, V. D. *Teor. Éksp. Khim.* **2000**, *36*, 63.

(7) Heyding, R. D.; Murray, R. M. *Can. J. Chem.* **1976**, *54*, 841.

(8) (a) Hiroto, U. *Jpn. Kokai Tokkyo Koho* JP, 01, 298 010, 1989. (b) Lakshmikumar, S. T. *Mater. Solut. Cells* **1994**, *32*, 7.

(9) Toyoji, H.; Hiroshi, Y. *Jpn. Kokai Tokkyo Koho* JP 02 173 622, 1990.

(10) (a) Korzhuev, A. A.; Kim, F. *Orab. Mater.* **1991**, *3*, 131. (b) Kainthla, R. C.; Pandya, D. K.; Chopra, K. L. *J. Electroanal. Chem.* **1980**, *2*, 127.

(11) (a) Yang, L. C.; Xiao, H. Z.; Shafarman, W. N.; Birkmire, R. W. *Sol. Energy Mater. Sol. Cells* **1995**, *36*, 445. (b) Rockett, A.; Birkmire, R. W. *J. Appl. Phys.* **1991**, *70*, R81.

(12) Zanio, K. In *Semiconductors and Semimetals*, *vol. 13: Cadmium telluride;* Willardson, R. K., Beer, A. C., Eds.; Academic Press: New York, 1978; Chapter 3.

(13) (a) Klimov, V. I.; Mikhailovsky, A. A.; Xu, S.; Malko, A.; Hollingsworth, J. A.; Leatherdale, C. A.; Eisler, H. J.; Bawendi, M. G. *Science* **2000**, *290*, 314. (b) Kim, J. H.; Kim, H.; Cho, K.; Kim, S. *Solid State Commun.* **2005**, *136*, 220.

(14) Durose, K.; Edwards, P. R.; Halliday, D. P. *J. Cryst. Growth* **1999**, *197*, 733.

(15) Wang, D. S.; He, J. B.; Rosenzweig, N.; Rosenzweig, Z. *Nano Lett.* **2004**, *4*, 409.

(16) Choi, S. H.; Kim, E. G.; Hyeon, T. *J. Am. Chem. Soc.* **2006**, *128*, 2520.

(17) Zhang, H.; Wang, L.; Xiong, H.; Hu, L.; Yang, B.; Li, W. *Adv. Mater.* **2003**, *15*, 1712.

(18) Lakshmi, M.; Bindu, K.; Bini, S.; Vijayakumar, K. P.; Sudha, Kartha, C.; Abe, T.; Kashiwaba, Y. *Thin Solid Films* **2001**, *386*, 127.

(19) Gerbec, J. A.; Magana, D.; Washington, A.; Strouse, G. F. *J. Am. Chem. Soc.* **2005**, *127*, 15791.

(20) (a) Choi, S. H.; Kim, E. G.; Park, J.; An, K.; Lee, N.; Kim, S. C.; Hyeon, T. *J. Phys. Chem. B* **2005**, *109*, 14792. (b) Puntes, V. F.; Krishnan, K.; Alivisatos, A. P. *Top. Catal.* **2002**, *19*, 145.

(21) (a) Pejova, B.; Grozdanov, I. *J. Solid State Chem.* **2001**, *158*, 49. (b) Lakshmi, M.; Bindu, K.; Bini, S.; Vijayakumar, K. P.; Kartha, C. S.; Abe, T.; Kashiwa, Y. *Thin Solid Films* **2000**, *370*, 89.